# NRC Publications Archive
# Archives des publications du CNRC

**Transient particulate matter measurements from the exhaust of a direct injection spark ignition automobile**

Smallwood, Gregory J.; Snelling, David R.; Gülder, Ömer L.; Clavel, Dan; Gareau, Daniel; Sawchuk, Robert A.; Graham, Lisa

**NRC Publications Archive Record / Notice des Archives des publications du CNRC :**
https://nrc-publications.canada.ca/eng/view/object/?id=22571b32-4274-4b66-8c98-0a68a1b208e9
https://publications-cnrc.canada.ca/fra/voir/objet/?id=22571b32-4274-4b66-8c98-0a68a1b208e9

**Questions?** Contact the NRC Publications Archive team at
PublicationsArchive-ArchivesPublications@nrc-cnrc.gc.ca. If you wish to email the authors directly, please see the first page of the publication for their contact information.

**Vous avez des questions?** Nous pouvons vous aider. Pour communiquer directement avec un auteur, consultez la première page de la revue dans laquelle son article a été publié afin de trouver ses coordonnées. Si vous n'arrivez pas à les repérer, communiquez avec nous à PublicationsArchive-ArchivesPublications@nrc-cnrc.gc.ca.

National Research Council Canada    Conseil national de recherches Canada

# CISTI    ICIST

Document Delivery Service
in partnership with the **Canadian Agriculture Library**

Service de fourniture de Documents
en collaboration avec **la Bibliothèque canadienne de l'agriculture**

## THIS IS NOT AN INVOICE / CECI N'EST PAS UNE FACTURE

MARIA CLANCY
DGO
INST FOR CHEM PROCESS & ENVIR TECH
NATIONAL RESEARCH COUNCIL CANADA
M-12, ROOM 141, 1200 MONTREAL RD.
OTTAWA, ON K1A 0R6
CANADA

| | |
|---|---|
| **ORDER NUMBER:** | CI-07808931-3 |
| **Account Number:** | WR001844 |
| **Delivery Mode:** | XLB |
| **Delivery Address:** | |
| **Submitted:** | 2009/03/24 15:49:02 |
| **Received:** | 2009/03/24 15:49:02 |
| **Printed:** | 2009/03/25 20:37:27 |

| Extended | Periodical | Virtual Lib. Blank form | CANADA |
|---|---|---|---|

| | |
|---|---|
| Client Number: | MARIA E. CLANCY |
| **Title:** | **SAE PAPER NO. 2001-01-3581** |
| Date: | 2001 |
| Article Title: | TRANSIENT PARTICULATE MATTER MEASUREMENTS FROM THE EXHAUST OF A DIRECT INJECTION SPARK IGNITION AUTOMOBILE |
| Article Author: | SMALLWOOD, G.J. ET AL. |

INSTRUCTIONS:   NEEDED BY: 17 APRIL 2009

Estimated cost for this 15 page document: $0 document supply fee + $0 copyright = $0

# Transient Particulate Matter Measurements from the Exhaust of a Direct Injection Spark Ignition Automobile

**Gregory J. Smallwood, David R. Snelling, Ömer L. Gülder, Dan Clavel, Daniel Gareau and Robert A. Sawchuk**
National Research Council Canada, ICPET Combustion Research Group

**Lisa Graham**
Environment Canada, Emissions Research and Measurement

## ABSTRACT

Diesel and gasoline engines face tightening particulate matter emissions regulations due to the environmental and health effects attributed to these emissions. There is increasing demand for measuring not only the concentration, but also the size distribution of the particulates. Laser-induced incandescence has emerged as a promising technique for measuring spatially and temporally resolved soot volume fraction and size. Laser-induced incandescence has orders of magnitude more sensitivity than the gravimetric technique, and thus offers the promise of real-time measurements and adds information on the increasingly desirable size and morphology information. Quantitative LII is shown to provide a sensitive, precise, and repeatable measure of the soot concentration over a wide measurement range.

The current research determined the tailpipe particulate emissions characteristics from a DISI (direct injection spark ignition) vehicle, including identifying the relative contributions of various engine modes to the total particulate emissions. The volume concentration measurements were obtained in the undilute exhaust with laser-induced incandescence (LII). Particulate measurements were also performed with ELPI instrumentation, sampling from a mini-diluter. Gravimetric filter sampling was performed to measure mass emission rate, organic/elemental carbon, and sulphates/nitrates/trace elements.

The LII technique was demonstrated to be capable of real-time particulate matter measurements over all vehicle transient conditions. The wide measurement range and lower detection limit of LII make it a potentially preferred standard instrument for soot measurements.

## INTRODUCTION

From an environmental perspective, there is an urgent need to decrease the total emissions from transportation engines. The undesirable exhaust emissions include CO, $CO_2$, $NO_x$, HC, and particulate matter (PM). $CO_2$ is a recognized greenhouse gas, and as a result of the Kyoto Protocol, industrialized countries have committed to reducing emissions of $CO_2$. This can be primarily achieved by reductions in fuel consumption, and direct injection spark ignition (DISI) engines offer substantially improved efficiency for gasoline-fueled vehicles. The concession is that the emissions reduction systems for other pollutants are not as well developed for these lean burn stratified combustion engines as they are for conventional port fuel injected homogeneous charge engines.

Demand for improved environmental performance has led to increasingly restrictive emission regulations for vehicles throughout Europe, North America, and Japan. Proposed regulations indicate that this trend to lower emissions levels will continue for the foreseeable future. Although PM is currently regulated only for diesel vehicles, future regulations will limit PM for all light duty vehicles. While PM is regulated for environmental and health concerns, there is also a strong need to control soot and other particulates in the exhaust plume because of their adverse influence on the performance of the power generation systems.

Efforts have focused on reducing the mass of the combustion-generated particulates in the larger $PM_{10}$ size range (weight of particulate mass below 10 μm aerodynamic diameter) which were visible and hence, readily associated with emissions at the source.
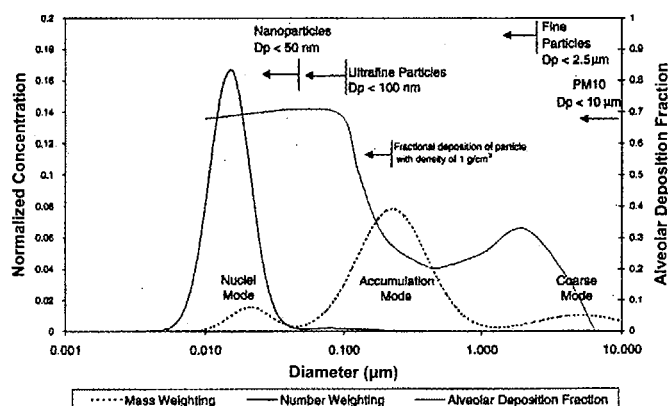
Figure 1: Conceptual engine exhaust particle size distribution [3].



Figure 2: Diesel engine exhaust particle size distribution as measured by SMPS [5].

However, especially deleterious are the small sized respirable aerosols and particulate matter that are known to produce adverse health effects and are suspected of producing high altitude clouds which adversely affect the earth's climatology [1, 2]. $PM_{2.5}$ range (weight of particulate mass below 2.5 μm aerodynamic diameter) particulates have recently been advanced as the regulatory standard for ambient particulates in the U.S. Future regulations may be established for $PM_{1.0}$. It is known that particles in the 0.3 μm size range deposit in the lungs and particles smaller than 0.3 μm find their way into the alveoli. Irrespective of their chemical composition, recent evidence indicates that these fine particles have harmful effects. Vehicle emissions data show that the majority of the particles fall in the range of 0.1 μm, as illustrated in Figure 1. However, it is the larger particles, centered around 0.3 μm, that dominate the mass-weighted size distribution [3].

Many different terms are used to describe emitted aerosols. Herein, PM refers to all solid particles and liquid droplets suspended in a gas. Soot refers to elemental carbon based particles emitted from combustion sources without adsorbed hydrocarbons.

To develop processes and techniques for limiting the emission of soot, we must first possess suitable means for reliably measuring various soot-related parameters. These methods must have adequate measurement range in order to be able to monitor and characterize the pollutant emissions over a very wide range of concentrations and must operate under a range of environmental conditions from *in situ* exhaust to atmospheric monitoring. In the case of particulate matter, information on the particle mass, size, and volume fraction is needed. The lack of availability of suitable diagnostics has resulted in a degree of uncertainty in the correlation of the particulate loading with health effects. Improvements in the instrumentation are needed to help in developing the test protocols, standards and regulations that will preserve the environment and limit risks to health.
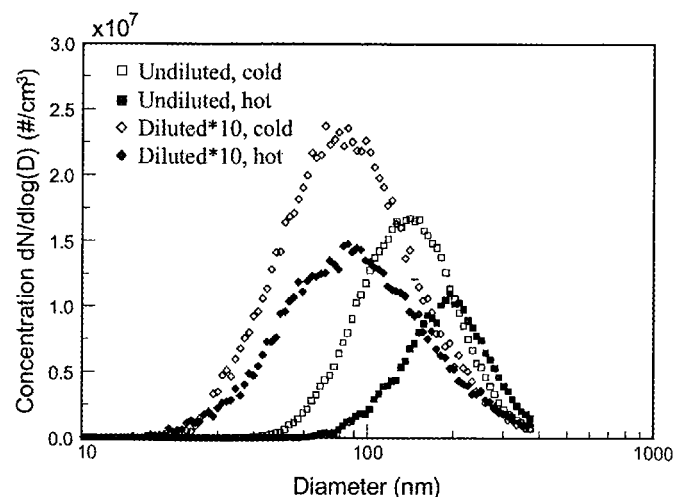
Laser-induced incandescence has emerged as a technique for measuring soot concentration and size, as non-soot matter is evaporated and/or does not contribute to the signal.

SAMPLING AND MEASUREMENT ISSUES

Concerns regarding dilution ratio, residence time, temperature, preconditioning, sampling line materials, and the instruments to measure particulates are being voiced with increasing frequency. Many of the issues have been recently summarized by Witze [4]. Residence time and gas temperature can have a significant impact on the formation rates of particulates, as well as dilution itself. The impacts of dilution and of heating both the diluent gas and the diluter body on particulate number and distribution are shown in Figure 2.

The differences in measured particulate size distributions and/or mass due to these sampling issues are attributed to marked variations in the quantity of condensed aerosols, and it is generally accepted that the measurement of soot is not sensitive to the sampling conditions. Recent evidence has indicated that soot emissions have characteristic size distributions which could be used to distinguish them from other aerosols [6].

Although there is little particulate data reported for DISI vehicles under transient conditions, there is some relevant work in the literature. Time-resolved ELPI (electrical low pressure cascade impactor) measurements for the US EPA FTP (Federal Test Protocol) driving cycle were reported for a diesel vehicle, in which the total number of particles appeared to follow the vehicle speed, not acceleration or deceleration [7]. Steady-state DISI particulates measurements have been performed [8], in which particular vehicle speeds produced dramatically different particulate behaviors (steady, highly fluctuating, and periodically fluctuating) which were attributed to the engine control system.

SMPS (scanning mobility particle sizer) data, collected in the 75 nm size bin for the first 500 s of the cold start FTP cycle for a DISI vehicle [9], indicated that there was a strong correlation between PM emissions and vehicle acceleration, as for conventional port fuel injected engines, and also with changes from homogeneous to stratified operation. Further comparison of DISI particulates data for 25 nm, 50nm, and 100nm SMPS size bins was performed over the ECE/EUDC combined driving cycles [10], indicating particle production was occurring during the stratified, globally lean, operation of the engine.

## LII BACKGROUND

Laser-induced incandescence (LII) measurement is a reliable means for spatially and temporally measuring the concentration of soot and the spherule size. Eckbreth [11] recognized the concept while working with Raman spectroscopy in flames and was troubled by the presence of soot particles that produced laser-modulated incandescence. Melton [12] performed numerical calculations to investigate the possibility of developing a soot diagnostic based on this laser heating of particles. He concluded that it might be possible to obtain the particle temperature, soot primary particle size distribution parameters, and relative soot volume fraction. Dasch [13] modeled the vaporization of small soot particles and conducted experiments demonstrating the method. Since that time, a number of research teams have investigated the method with varying degrees of success [14-22]. Dec et al. [15] used the incandescence method to visualize the soot production inside a diesel engine.

With the LII method, the soot within the laser beam path is heated rapidly using a pulsed laser source with duration typically less than 20 ns (FWHM). The soot is conventionally heated from the local ambient soot temperature to the soot vaporization temperature (approximately 4000 to 4500 K). The incandescence from the soot particles is measured using collection optics and photodetectors. Using appropriate calibration and analysis of the incandescence signal, information on the soot volume fraction and primary soot particle size may be obtained. Laser energy absorption by the soot particles and the subsequent cooling processes involve complex analysis of the nano-scale heat and mass transfer in time and space [23, 24]. The method is essentially nonintrusive and is capable of making in situ measurements over a very large range of soot concentrations in both flames and under ambient conditions. However, it is not completely non-perturbing as the laser heating can be expected to affect the soot morphology [25] and cause some evaporation during the short duty cycle of the laser.

LII can fill the need for soot particulate measurements since the LII signal is proportional to soot volume fraction over a wide measurement range. However, LII provides a relative measure of soot concentrations and requires a calibration for quantification of soot particulate concentrations. Currently, calibration of the technique for absolute soot particulate concentrations may be made by comparison of the LII signal to a system with a known soot volume fraction determined through traditional methods [26]. Using empirical calibration procedures, LII has been used to measure soot particle volume fraction in steady-state and time-varying diffusion flames, premixed flames, within engines [27] and in diesel engine exhaust streams [28] and gas turbine exhausts [29]. Recently, a novel technique for performing absolute light intensity measurements in LII has been presented, thus avoiding the need for a calibration in a source of soot particulates with a known concentration [30, 31], and thus extending the capabilities of LII for making practical quantitative measurements of soot. Using this in situ absolute intensity self-calibration technique, LII has been applied to measure soot particle volume fraction in laminar diffusion flames [31], carbon black [31, 32] and in diesel engine exhaust streams [31, 33, 34].
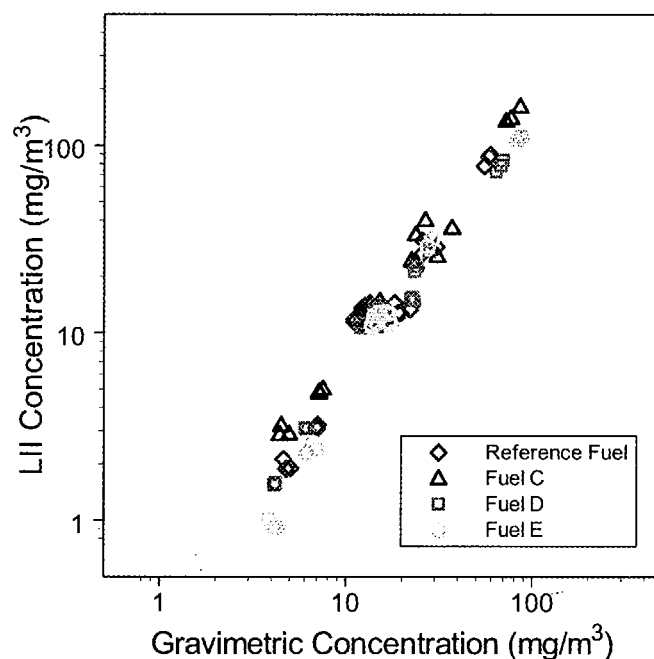


Figure 3: Engine out emissions for four diesel fuels at eight steady-state modes simulating the EPA heavy duty transient test procedure. The gravimetric filter sampling and the LII measurements were performed on the same sample stream concurrently [35].

Table 1: Brake Specific Emissions by Fuel Type [35].

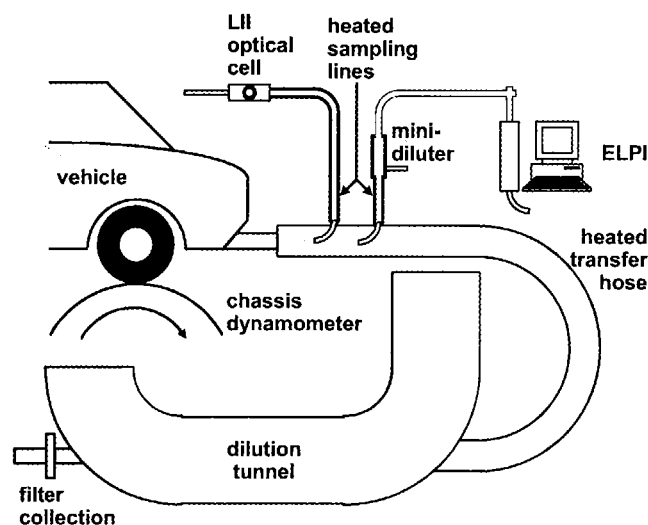| Fuel | Sulphur (ppm) | Gravimetric PM BSE (g/hp·hr) | LII soot BSE (g/hp·hr) |
|---|---|---|---|
| Reference | 192 | 0.074 | 0.074 |
| Fuel C | 184 | 0.087 | 0.092 |
| Fuel D | 46 | 0.082 | 0.070 |
| Fuel E | 32 | 0.084 | 0.074 |

Figure 4: Schematic of sampling apparatus and particulate measurement instrumentation.

With further refinement of the algorithms and improved knowledge of the probe volume characteristics, we have revisited the data for heavy duty diesel particulate emissions that was previously published [34]. The revised engine out (undilute) emissions for four fuels [35] are shown in Figure 3. As can be seen in Figure 3, the correlation between LII and the standard gravimetric technique is excellent.

The revised brake specific emissions (BSE) for the EPA heavy duty transient test procedure are summarized in Table 1. As before, the LII results show same trends as the gravimetric results, with the soot BSE increasing from the reference fuel to Fuel C for the higher sulphur fuels, and from Fuel D to Fuel E for the lower sulphur fuels. The agreement between the two methods is now much closer. However, some differences do remain. The fact that LII measures lower quantities for soot BSE than gravimetric technique for fuels D and E emphasizes that LII and the gravimetric techniques are measuring different properties of the particulates.

## EXPERIMENTAL

### VEHICLE AND DRIVING CYCLES

A state-of-the-art production direct injection spark ignition engined vehicle from the Japanese market was used as the evaluation platform for this research. This vehicle uses a lean-burn stratified charge combustion concept for most of its operating modes. The vehicle was unmodified, and all emissions were measured from the tailpipe. The fuel for this work was indolene reference fuel (4 ppm sulfur).

The driving cycles performed were the Cold Start (CS) LA-4 transient driving cycle, the Hot Start (HS) LA-4 transient driving cycle, and the HWFET (highway fuel economy test) transient driving cycle. All three of these cycles were performed on each of two consecutive days.

The cold start LA-4, followed by a 10 minute break and then the first 505 seconds of the hot start LA-4, comprise the EPA standard FTP (Federal Test Procedure) transient driving cycle.

## EXHAUST EMISSION MEASUREMENTS

The research was performed on a chassis dynamometer normally used for regulatory compliance testing, equipped for EPA FTP emissions measurements. A schematic of the sampling layout is shown in Figure 4. A constant volume dilution tunnel was employed for regulated gaseous emissions and filter paper particulate collection. The gaseous emissions were bag collected and sampled for CO, $CO_2$, $NO_x$, and THC. Gravimetric filter sampling was performed to measure $PM_{2.5}$ mass emission rate and particle phase organic carbon/elemental carbon content, and to collect samples for sulphate / nitrate / trace elements content.

The samples for measuring organic/elemental carbon (OC-EC) content were analysed using the NIOSH 5040 thermal optical transmittance method, and were corrected for sampling artifact (OC deposited on EC filter). The total carbon (TC=OC+EC) should be less than $PM_{2.5}$ mass. Along with trace metals, sulphates, and bound water, the amount of hydrogen associated with the OC fraction is not included in the TC total. The sulphate / nitrate / trace elements content was determined by ion chromatography

Particulate size distributions were measured after sampling with a fixed dilution ratio Dekati mini-diluter. The samples were drawn from the heated transfer hose at a point within 1 m of the tailpipe exit, through a heated sample line (100°C), to the diluter. The stream was then split, and sent to a Dekati ELPI for the size distribution measurements. The ELPI provides data at 1 s intervals, but for a limited number (12 stages) of size bins.

As LII only measures the elemental carbon component of the particulates, dilution is not necessary. Other condensed materials, such as the organic fraction of the particulates and water, do not contribute to the signal measured by LII, and are typically evaporated by the high energy laser well before the significant portion of the LII signal is detected. The samples for LII were also drawn from the heated transfer hose at a point within 1 m of the tailpipe exit, through a 9.5 m heated sample line (107°C), to the optical cell, shown in Figure 5. The optical cell was heated to 75°C in order to prevent water vapor from condensing on the windows. The windows were monitored for contamination, but did not require cleaning, due to the low level of particulates being sampled and the aerodynamics through the cell. The exhaust gases were drawn through the cell at a constant 5 SLPM flow rate. This resulted in a transit time through the sample line of ~ 6 s. A similar transit time was estimated for the ELPI results.
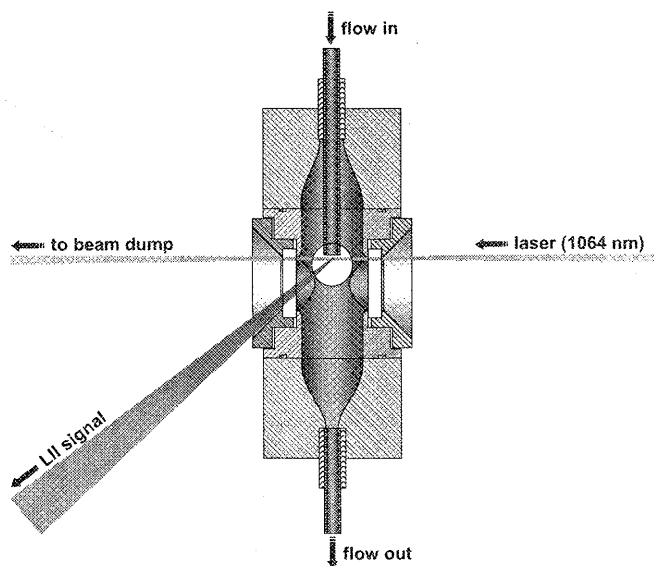
Figure 5: Sectional top view of optical cell for LII measurements.

## LII MEASUREMENT SYSTEM

A new LII system, shown in Figure 6, was configured for portability, such as this application. As the LII systems at NRC have been described previously [33, 34], details are provided primarily on the modifications made for these DISI exhaust particulate measurements. Briefly, a pulsed Nd:YAG laser, operating with 60 mJ/pulse at 20 Hz and 1064 nm, was used as the excitation source. A half-wave plate (to rotate the plane of polarization) in combination with a thin film polarizer (angle-tuned to transmit horizontally polarized radiation) was used to adjust the laser energy as required. A second half-wave plate was used to return the plane of polarization to vertical. Near top-hat profiles were used for all measurements to deliberately ensure that the soot particles were heated to a uniform temperature throughout the sample volume. The use of the absolute intensity approach [31] provides for continuous self-calibration of the LII technique, and allows use of lower laser fluences and lower maximum soot temperatures. Thus, issues associated with evaporating a significant portion of the soot are avoided. The absolute intensity method applies two-color pyrometry principles to determine the particle temperatures, relating the measured signals to the absolute sensitivity of the system as determined with a strip filament lamp.

The LII signal from the center of the laser beam was imaged at 1:1 magnification onto 2 mm diameter aperture, which was direct-coupled to a two-channel demultiplexer detector box. The imaging system was arranged such that the imaging axis was at an angle of 35° from the forward direction of the laser beam. Thus the sample volume in the flame was a slanted cylinder of diameter 2 mm whose mean length was 4.9 mm. This probe volume is significantly larger than that used for previous measurements, providing substantially improved sensitivity for the lower concentrations of soot anticipated from the DISI exhaust.
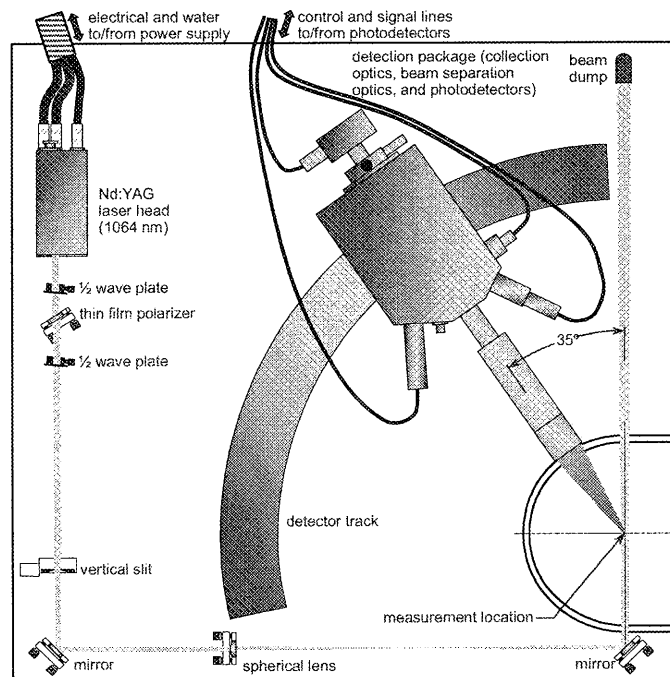


Figure 6: Top-view schematic of the LII optical apparatus.

The LII signal was recorded by two photomultipliers, equipped with narrowband interference filters centered at 400 nm and 780 nm, respectively. Transient signals from the photomultipliers were recorded and subsequently transferred to a computer for further analysis. Multipulse averages were acquired with 40 samples per average providing data at 2 s intervals, unless otherwise noted. Use of a higher repetition rate laser could provide greater temporal response. Alternatively, fewer pulses could be averaged, at the cost of increased noise, to improve the temporal response.

## RESULTS

The gaseous emissions and gravimetric filter emissions are presented, followed by the LII results, the ELPI results, and a comparison of the LII results to the ELPI results. Data for two complete trials was collected on consecutive days.

### GASEOUS / PARTICULATE FILTER MEASUREMENTS

As the data was collected for both cold and hot start LA-4 cycles, there were four emission bags available (first 505 s and subsequent 864 s for each of cold and hot start). The first three were combined to provide the EPA FTP test procedure. Results for all four individual phases, the combinations of the first three and all four, and the HWFET are shown in Figure 7 for CO, $CO_2$, $NO_x$, and THC. The $CO_2$, $NO_x$, and THC remained consistent from the first trial to the second. However, the CO concentration showed a marked decrease of 27% for the EPA FTP cycle between trials. As expected, the bulk of the THC emissions were produced during the cold start phase.
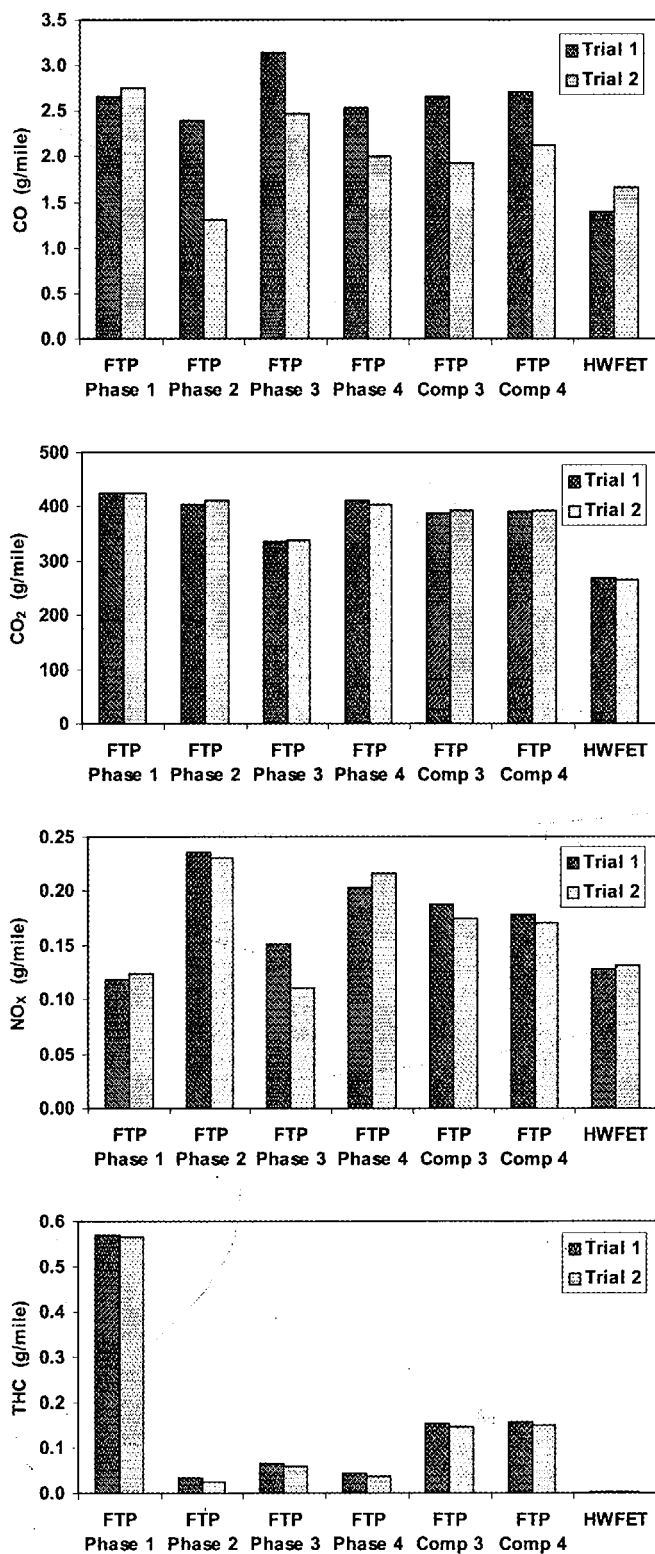
657

Figure 7: Gaseous emissions of CO, $CO_2$, $NO_x$, and THC from a DISI vehicle. FTP Phase 1 and 2 represent a cold start LA-4 transient cycle, FTP Phase 3 and 4 represent a hot start LA-4 transient cycle, FTP Comp 3 is the average of the first three FTP phases, FTP Comp 4 is the average of all four phases, and HWFET is the highway fuel economy test.
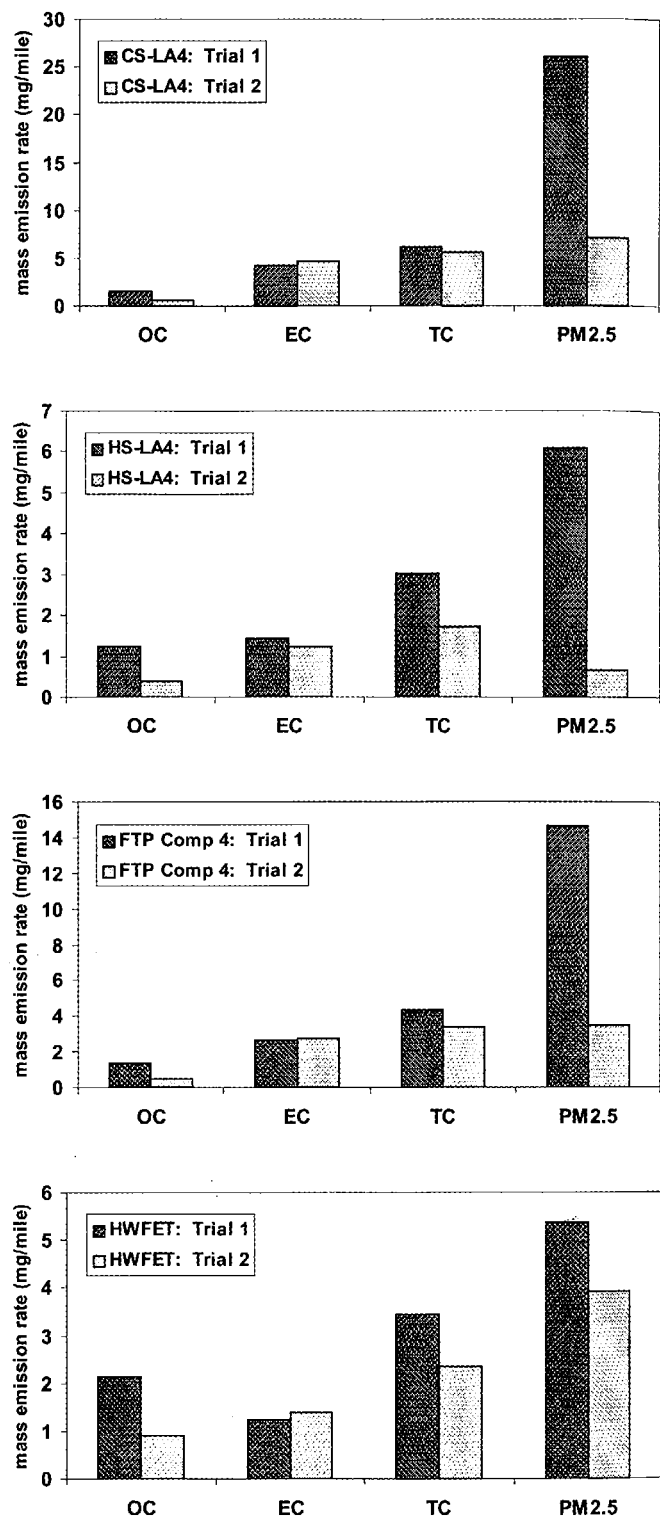
Figure 8: Particulate mass emissions rates from a DISI vehicle. OC, EC, and TC represent the organic, elemental, and total carbon, respectively, and $PM_{2.5}$ represents the total particulates below 2.5 μm. CS-LA4 and HS-LA4 represent cold and hot start LA-4 transient cycles, respectively, FTP Comp 4 is the average of the CS-LA4 and HS-LA4, and HWFET is the highway fuel economy test.

Gravimetric filter data was collected once per cycle, and the cold and hot start data were combined, as shown in Figure 8 for the mass emission rates. As expected, the bulk of the THC and PM emissions were produced during the cold start phase. The $PM_{2.5}$ mass emission rate as measured by the gravimetric technique also showed a marked decrease between trials.

For the cold start, hot start, and HWFET tests, the OC had a marked decrease between trials, while the EC had little variation. For the total carbon, the Trial 2 cold start measurement is nearly the same as $PM_{2.5}$ mass, which is the expected result. The $PM_{2.5}$ mass for the Trial 1 cold start is much greater than TC, suggesting something other than a carbon-based species is present, or that there was an error in handling the filter. For the hot start cycle, TC is much less than $PM_{2.5}$ mass for Trial 1, while for Trial 2 TC is greater than the $PM_{2.5}$ mass. As the latter result appears inconsistent, again there may have been an error in handling one of the filters. The difference in the two TC results for the two days is a result of the OC being greater for Trial 1. For the HWFET cycles, the TC masses are less than the $PM_{2.5}$ masses on both days. The difference in the two TC results for the two days is a result of the OC being greater on the first day.

The only ions found in measurable quantities were nitrate and sulphate ions, which were both near the minimum quantitation limit for all trials. The sulphate emission rate is low as the vehicle was running on a very low sulphur fuel. The measured emissions of $SO_2$ were below the detection limits of the method for all tests.

## LII PARTICULATE MEASUREMENTS

Typically, LII is performed with a single point calibration in a source of known concentration of particles. The intensities measured in a changing environment are then peak signal scaled back to the calibrated measurement to obtain a quantitative measure of concentration. This method is somewhat sensitive to the initial temperature of the particulates, the size and morphology of the aggregates, and the composition of the surrounding gases. Thus, the calibration should be performed with the same particulates that are to be measured, under the same environmental conditions. Use of excessive laser fluence reduces this sensitivity, at the cost of increased evaporation rates. Use of the absolute intensity method provides an *in situ* continuous self-calibration, which in turn allows low fluence excitation of the particulates, minimizing the evaporation and eliminating sensitivity to the nature of the particulates and their environment.

The difference between peak signal scaling (single point calibration) and continuous self-calibration is demonstrated in Figure 9. The vehicle speed for the LA-4 driving cycle is shown at the bottom, and the results for the two analysis methods are shown at the top, where the self-calibration method is referred to as full LII analysis (since the absolute intensity is calculated for every datum of each measurement).
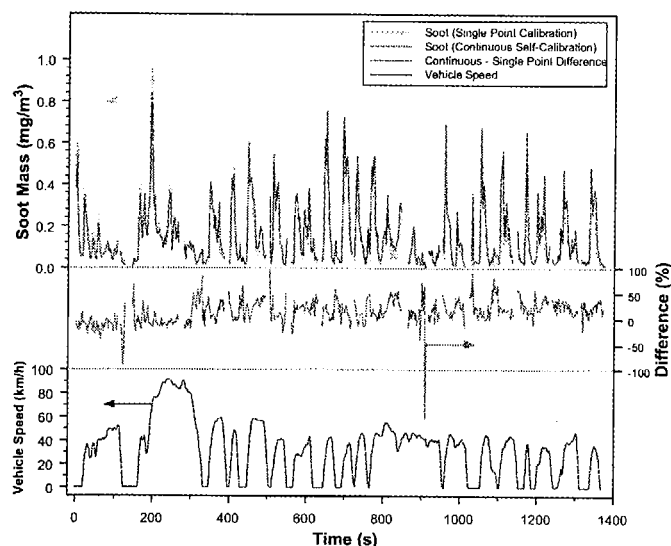


Figure 9: Comparison of peak signal scaling and full absolute intensity calibration methods for LII derived soot mass (top); relative soot mass for the two methods (middle); and target vehicle speed during LA-4 transient cycle (bottom).
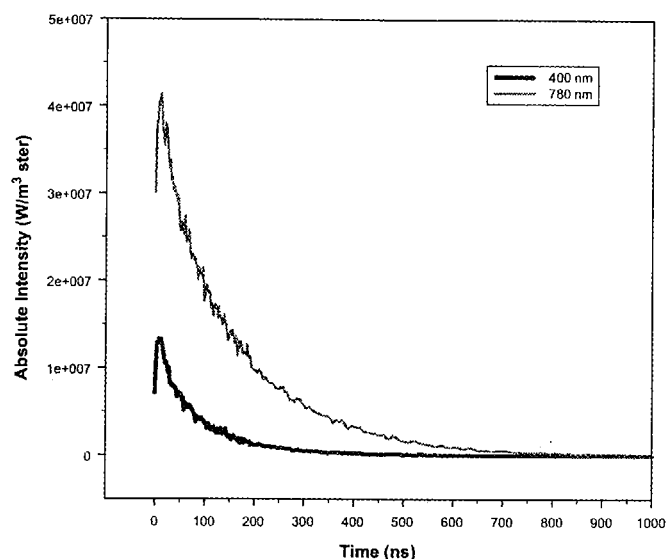


Figure 10: Typical LII signals for 400 nm and 780 nm channels for a single acquisition, illustrating signal quality for moderate concentration (400 ppt) decays as particles cool within 1 μs.

Although the two methods provide similar results, the latter offers the advantage that it is calibrated to the particulate temperature for every acquisition. The greatest difference between the methods occurs at times when the soot mass is at a minimum, as the minor differences between two small quantities are amplified. This is dependent on the choice of conditions for which the calibration is performed for the peak signal scaling method. All further LII data presented is determined by the full absolute intensity calibration method for each data acquisition.
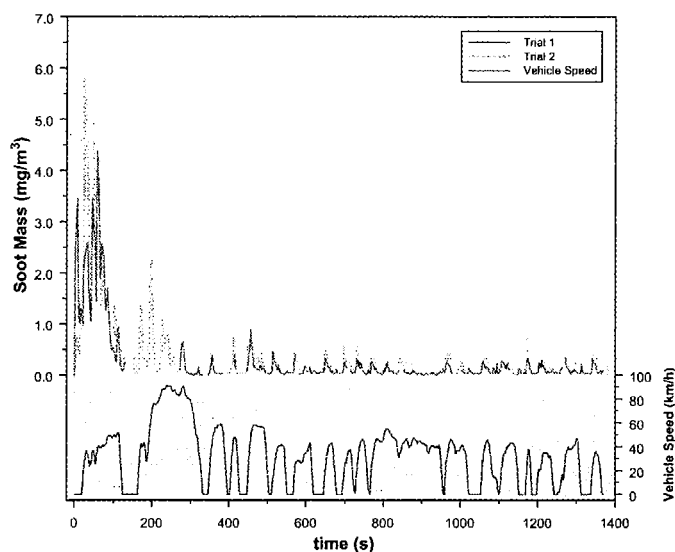
Figure 11: Comparison of cold start LA-4 transient cycle soot mass emissions as determined by LII for two separate trials (top) and vehicle speed during LA-4 transient cycle (bottom).
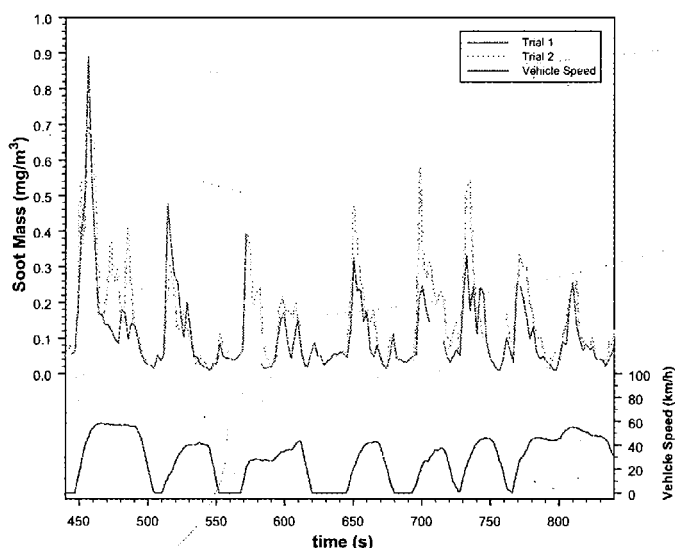


Figure 12  Comparison of cold start LA-4 transient cycle soot mass emissions as determined by LII for two separate trials (top) and vehicle speed during LA-4 transient cycle (bottom) (detail from Figure 11).

The LII data acquisition system suffered occasional interruptions, as can be observed from the results shown in Figure 9. This was due to an issue with the data acquisition software in use at the time.

For the lower maximum particulate temperatures achieved with low fluence irradiation, and the relatively cool gas temperatures, the rise and decay of the LII signal is typically over within 1 μs. This can be observed in Figure 10, where the signal from the 400 nm channel is seen to rise to a lower peak intensity and decay more rapidly than the signal from the 780 nm channel, as would be expected for black-body radiation. Although

the soot concentration for the data shown in Figure 10 was only 400 ppt (0.76 mg/m$^3$), is can be seen that the signal-to-noise ratio is more than adequate to provide high quality data. Concentrations below 5 ppt (0.01 mg/m$^3$) were measured frequently with sufficient precision during these experiments. As noted earlier, sensitivity for LII is only limited by the probe volume dimensions and the available laser energy.

The LII measurement of soot mass emission rates for two cold start LA-4 trials on consecutive days is shown in Figure 11. The greatest mass emission rates occur during the first 250 s of this cycle, during which the engine and emissions systems are warming up. The large gap in the data for Trial 1 between 140 and 280 s was due to the issues with the data acquisition software. Throughout the cycle, the increased mass emission rate episodes for this vehicle appear to correspond to the acceleration phases. This is shown in Figure 12, where the timing of the particulate events is demonstrated to coincide with the acceleration phases of the driving cycle. After the warm-up period, deceleration and cruising produce minimal levels of soot, and even under acceleration, the levels do not reach 1 mg/m$^3$. Although there is significant variation in the soot emissions on a trial-to-trial basis, the results clearly track each other and the transients in the driving cycle.

Similar results were found for the hot start LA-4 driving cycle, with the exception that the high soot levels during the first 250 s were not present, as the vehicle was already warmed up. This is shown in Figure 13, with an expanded vertical axis as compared to Figure 11. At no point do the soot levels reach 1 mg/m$^3$.

For the highway fuel economy test, Figure 14, moderate soot levels of an average 0.2 mg/m$^3$ were recorded by LII, with occasional peaks due to acceleration. Again, at no point do the soot levels reach 1 mg/m$^3$. During the second trial, 100 pulse averages were recorded after 125 s, providing reduced temporal resolution of 5 s. This can be observed in Figure 14, where the second trial data displays far less structure than the first trial data at times after 125 s. If more temporal resolution is desired than the 2 s shown for the first trial, the number of pulses averaged could be reduced at the expense of increased noise in the signal.

In general, the second trials produced higher levels of soot, which could be due to a number of factors, such as changes in the environmental conditions or variations in the driver performance from one day to the next. The mean concentration measured by LII was 31% less for the hot start Trial 1 than for Trial 2. The differences were substantially less for the cold start trials (14% less) and slightly less for the HWFET trials (25% less). These differences are opposite to the PM$_{2.5}$ results, which decreased from Trial 1 to Trial 2. This is likely due to the different nature of the particles being measured. Note that this is a time average of the LII data, not a volume or mass average, so direct comparison to the filter measurements is not advised.
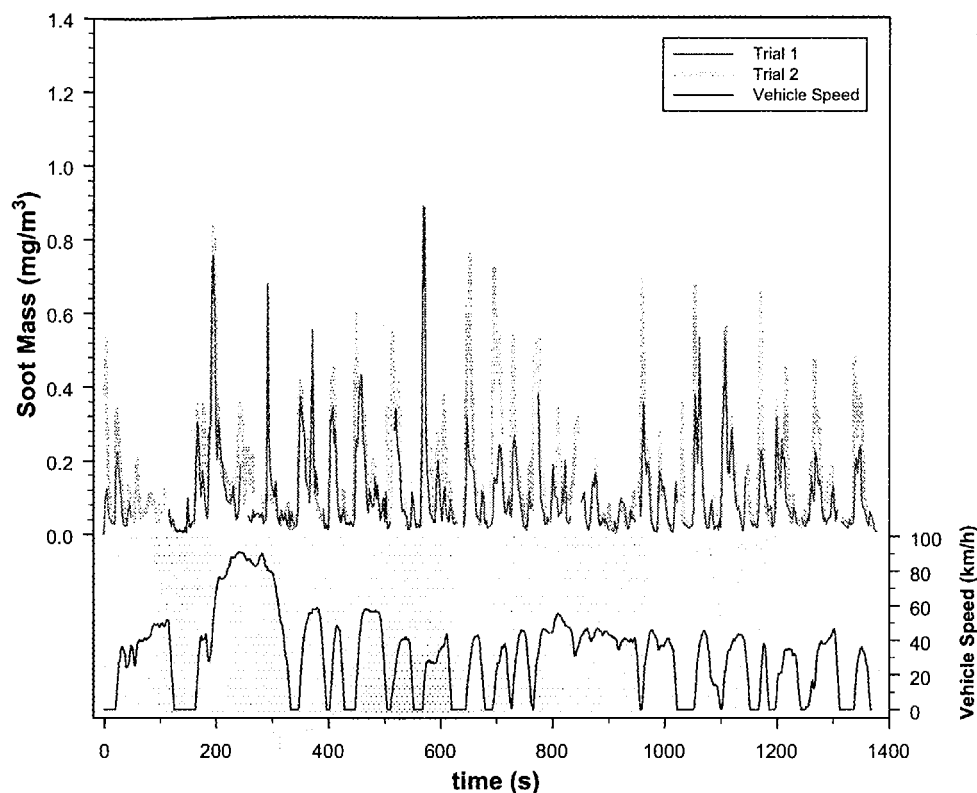
Figure 13: Comparison of hot start LA-4 transient cycle soot mass emissions as determined by LII for two separate trials (top) and vehicle speed during LA-4 transient cycle (bottom).
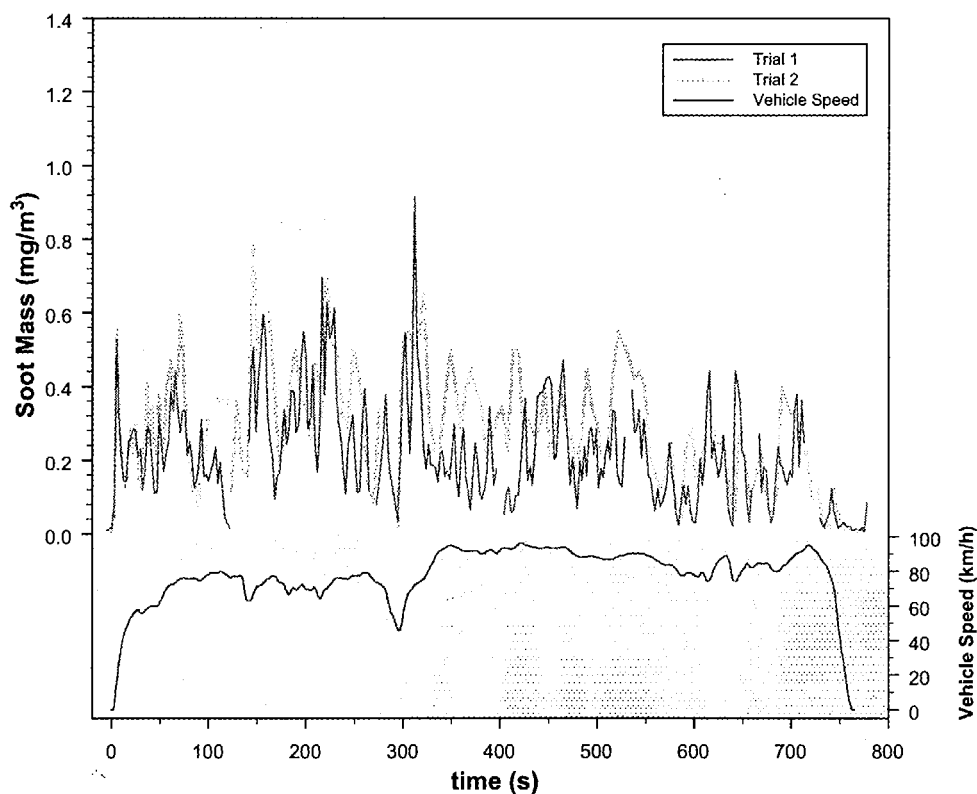


Figure 14: Comparison of HWFET transient cycle soot mass emissions as determined by LII for two separate trials (top) and vehicle speed during HWFET transient cycle (bottom). Note that after 125 s, data for Trial 2 is based on 5 s averages.
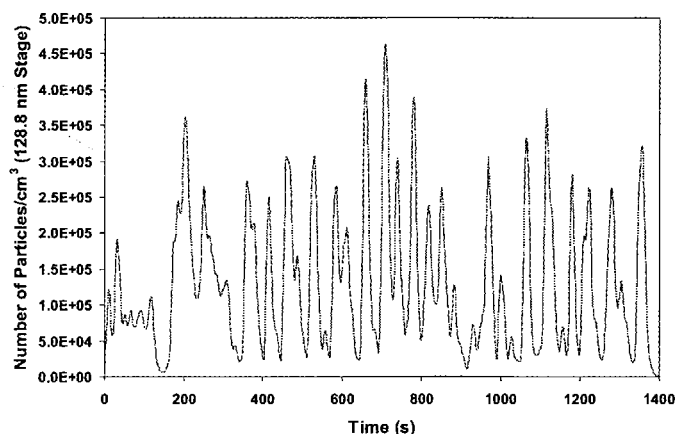
Figure 15:   Number concentration of particles as determined by ELPI for hot start LA-4 transient cycle. Data is for a single stage with a mid-point diameter of 128.8 nm.
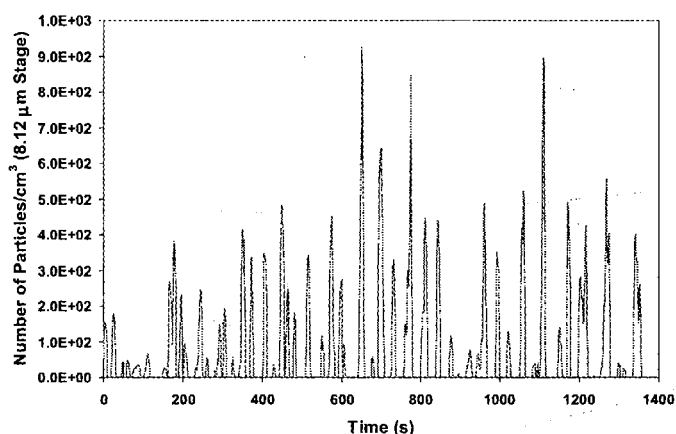


Figure 16:   Number concentration of particles as determined by ELPI for hot start LA-4 transient cycle. Data is for a single stage with a mid-point diameter of 8.12 μm.
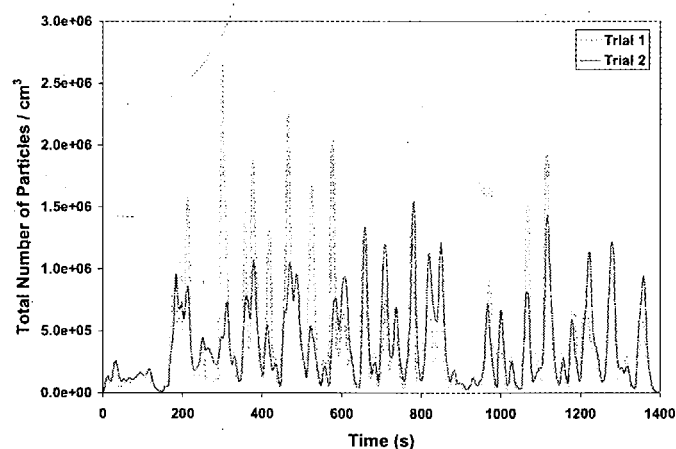


Figure 17:   Number concentration of particles as determined by ELPI for two separate hot start LA-4 transient cycle trials. Data is for all twelve stages combined.

## ELPI MEASUREMENTS

Due to cooling of the stream sampled by the ELPI instrument during the dilution process, the measured particulates are composed of condensable species, such as organics, water, and sulphuric acid, as well as the soot and trace elements present in an undilute stream. The ELPI instrument has a 1 s data acquisition rate, yet appears to have less time response than the LII system with 2 s intervals. This is likely due to the fact that the time taken to sweep the volume of the impactor is greater than 1 second. This instrument broadening can be observed by comparing the temporal structure in Figure 15 to that in Figure 13, where we have been able to show that the LII results exhibit finer detail. Although ELPI data was acquired during all trials, for the sake of brevity only results from the hot start LA-4 trials are presented. The mid-point diameters of the 12 stages for the ELPI vary in logarithmic progression from 41.7 nm to 8.12 μm. The results for the 128.8 nm stage are shown in Figure 15 and for the 8.12 μm stage are shown in Figure 16, where the number concentration of particulates shows similar behavior to that obtained by LII, with peaks occurring during the acceleration phases of the driving cycle. The particulates captured on the larger stages are unlikely to be combustion generated engine out particulates, and are more likely to be particles mechanically released from the walls of the exhaust system.

The results for all twelve stages were summed to provide the total number concentration of particulates during the driving cycle, as shown in Figure 17. Note that the total number of particles shows the same temporal variations as the smaller size single stage results. The results from the two trials show similar temporal behavior.
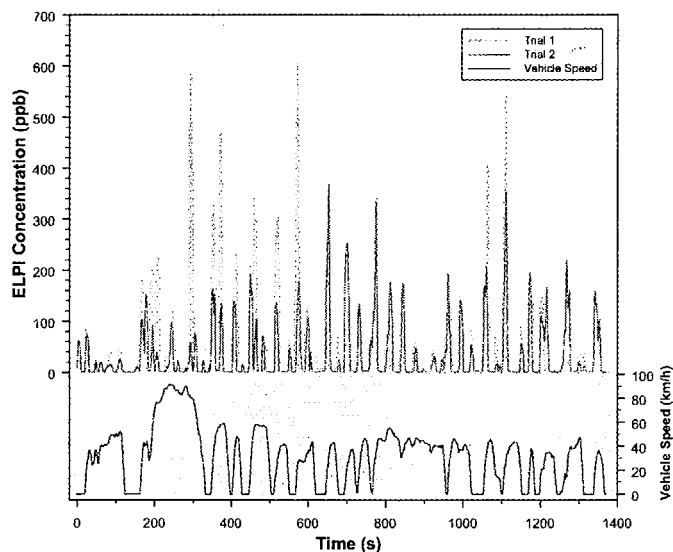


Figure 18:   Comparison of hot start LA-4 transient cycle particulate volume concentration emissions as determined by ELPI for two separate hot start LA-4 transient cycle trials. Data is for all twelve stages combined.
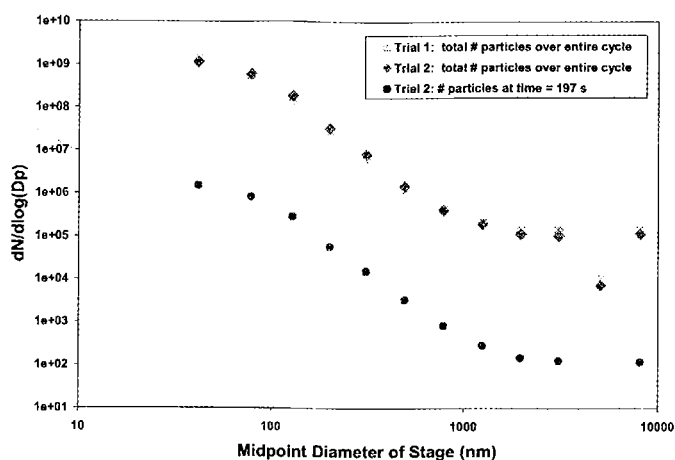
Figure 19: Size distribution of particles as determined by ELPI for the two hot start LA-4 transient cycle trials and for one time interval in Trial 2.

The volume concentration of particulates at each measurement time is shown in Figure 18, where we demonstrate that the volume more closely follows the large size single stage results shown in Figure 16. This is to be expected as the larger diameter particles, although fewer in number, represent proportionately more volume, and thus dominate the total volume measurement. The ELPI results also showed similar behavior in two consecutive trials, as shown in Figure 18. However, in contrast to the data obtained with LII, the volume concentration data from ELPI for the second day appeared less than the data for the first day. The difference from the LII data may be due to the fact that the ELPI instrument is measuring a different property than the LII system. The implication is that there were significantly more condensed organics in the first trial to more than offset the slight increase in elemental carbon matter observed in the second trial. The difference may also be due to the erratic performance of the 5.08 $\mu$m stage, as errors in the number of these large size particles has a disproportionate effect on the total volume. The total volume measured by ELPI was 27% greater for the hot start Trial 1 than for Trial 2. The differences were substantially less for the cold start trials (2 % less) and the HWFET trials (11 % greater).

The size distribution data for all twelve stages is shown in Figure 19, for both a single measurement time and summed over the entire duration of the LA-4 transient cycle. The two sets of data show the same distribution shape, indicating that there is little variation in the distribution over the duration of the cycle. The deficit observed in the data for the 5.08 $\mu$m stage was a cause for concern. In reviewing the ELPI data, this deficit appeared during all of the trials. This stage was far less responsive than the others, with much longer intervals with no signal to report. Instrument recalibration may be required. The Trial 1 and Trial 2 ELPI size distribution data appear similar.

## LII / ELPI COMPARISONS

Direct comparison of the soot concentration as determined by LII and the total volume of particles as determined by ELPI is presented in Figure 20. In a qualitative sense, these two properties appear to correlate well, as both follow the driving cycle transients with similar relative magnitudes. A detailed view of a portion of the data from Figure 20 is shown in Figure 21. The ELPI has a sensitivity threshold below which it reports zero signal, whereas LII is demonstrating its superior sensitivity, showing response at very low concentration levels. The greater temporal response of LII is also evident in Figure 21 as there is much more structure in the temporal profile of the LII concentration data. Although the two signals do show mostly similar features on a gross scale, there is a significant difference in response to the event at 195 s, with the ELPI showing far less response in comparison to some of the other peaks, whereas the LII indicates a much more significant response.

Further detail is shown in Figure 22, where we show that the peaks in particulate concentration are clearly aligned with the acceleration phases of the transient driving cycle, with minimal levels of particulate produced during steady-state and deceleration. Although the peaks for the two methods are aligned, LII shows considerably more detail in regions where ELPI has dropped below its sensitivity threshold.

## DISCUSSION

The results presented above indicate that the greatest level of soot is emitted during the acceleration phases of the driving cycles, with substantially lower levels emitted during steady speed driving and deceleration. Further investigation of the LII data supports these findings. The HWFET, which is dominated by relatively steady high speed driving, illustrates that there is little correlation between speed and soot mass emission rate, as shown in Figure 23. However, there appears to be a weak positive correlation between acceleration and soot mass emission rate, as shown in Figure 24. The data for the HWFET is biased, having more data at high speeds, and most of the data at or near zero acceleration.

To investigate the effect of acceleration, it is more interesting to inspect the data acquired during the LA-4 cycles, which are dominated by stop-start driving. Even so, the most frequent modes are at or near zero acceleration. The data for the cold start LA-4 cycle is presented in two parts: that which was significantly different from the hot start data, which was the first 250 s, and that which was similar to the hot start data, indicating a fully warmed engine and emissions system, for the period after 250 s. This data is presented in Figure 25, where the data for the first 250 s is generally much higher than the data after warm-up has occurred, and also shows little correlation with acceleration. However, Figure 25 also shows that for the cold start LA-4 cycle, after 250 s, there is a distinct positive correlation
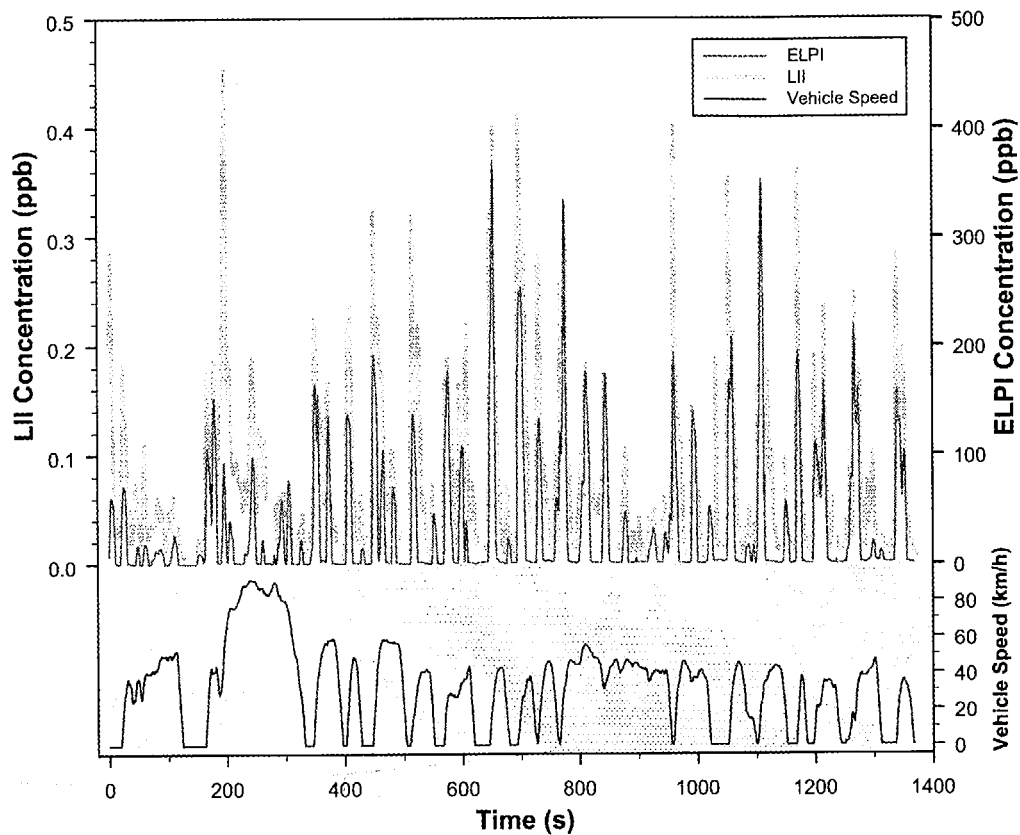
Figure 20: Comparison of levels of soot determined by LII and particulate determined by ELPI for hot start LA-4 transient cycle.
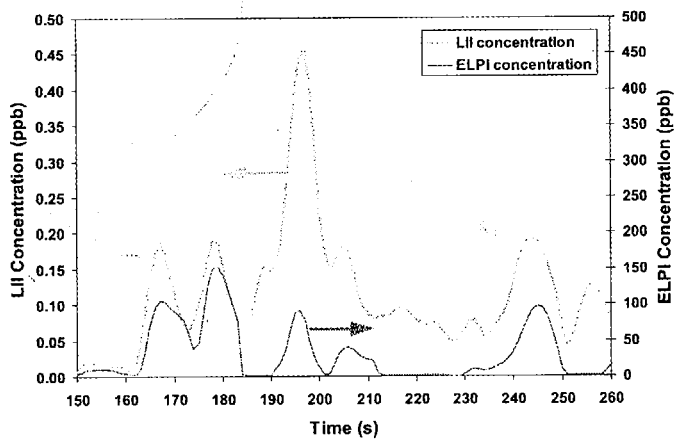


Figure 21: Detail from Figure 20 illustrating relative temporal response and sensitivity of LII and ELPI.
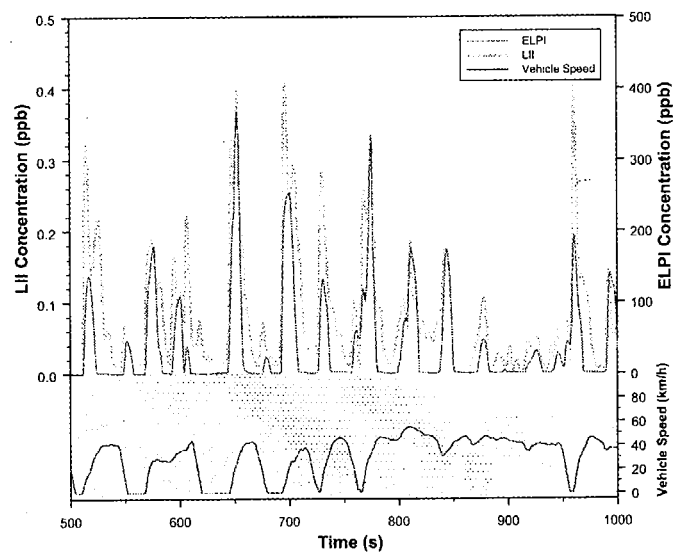


Figure 22: Detail from Figure 20 illustrating relative temporal response of LII and ELPI to vehicle speed, acceleration, and deceleration.
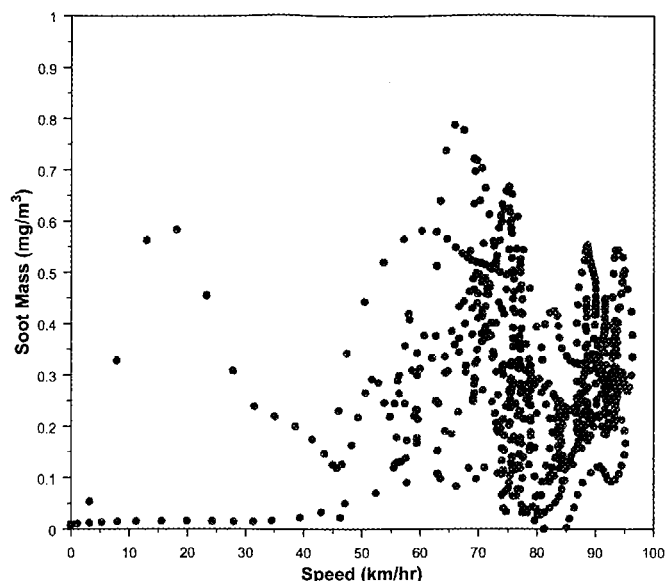
Figure 23: Soot mass concentration determined by LII versus speed during HWFET transient cycle.
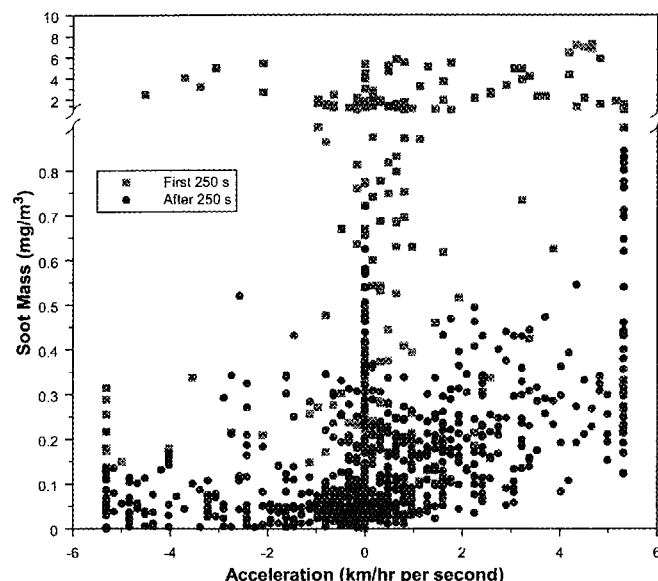


Figure 25: Soot mass concentration determined by LII versus acceleration during cold start LA-4 transient cycle.
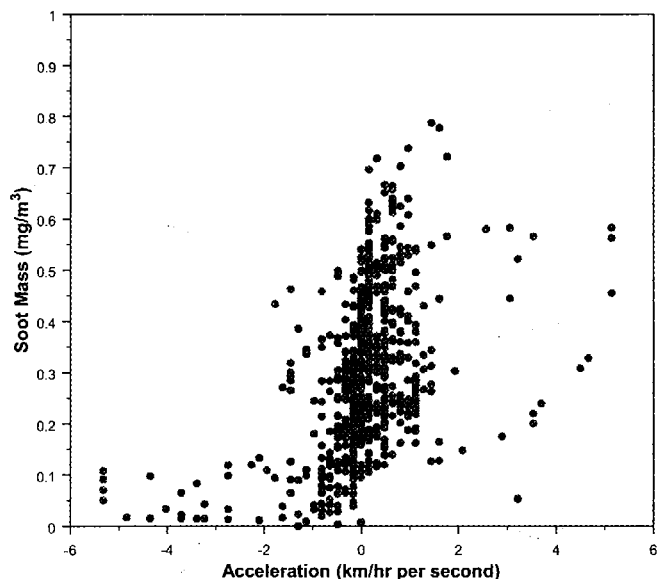


Figure 24: Soot mass concentration determined by LII versus acceleration during HWFET transient cycle.
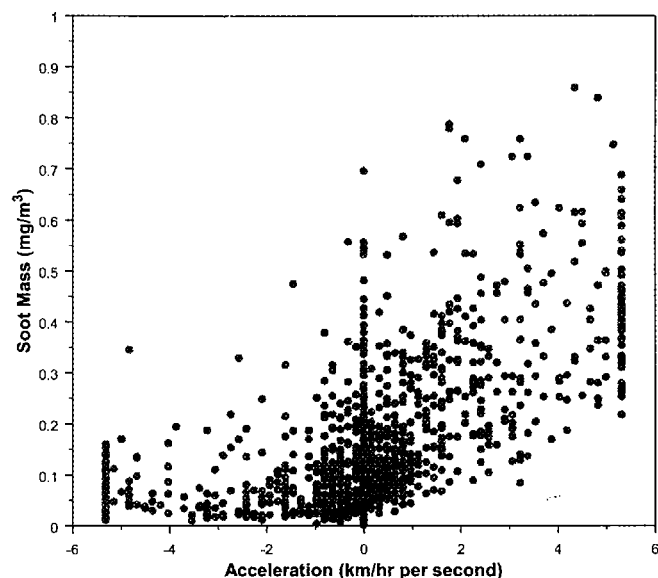


Figure 26: Soot mass concentration determined by LII versus acceleration during hot start LA-4 transient cycle.

between positive acceleration and soot mass emission rate, with little or no correlation for deceleration. This observation is even more apparent for the hot start LA-4 cycle, which was not split into two time periods. Figure 26 shows a similar, slightly more definitive, result for the relationship between acceleration and soot mass emission rate for the hot start LA-4 cycle.

## FUTURE WORK

To complete this study, the SMPS data that was acquired concurrently with the data presented herein will be analyzed and reported.

As stratified charge DISI vehicles use lean deNO$_x$ catalysts in the emission control systems, they are required to operate on low sulphur fuel. An upcoming study will investigate the effect of commercial gasolines (instead of indolene) with varying levels of sulphur (within the operational limits for the vehicle) on the particulate emissions.

Further development of the LII technique will include complementary scattering measurements interpreted with Rayleigh-Debye-Gans polydisperse fractal aggregate (RDG-PFA) theory [36] to determine characteristics of the aggregate size distributions and other properties of interest.

## SUMMARY AND CONCLUSIONS

The tailpipe particulate emissions from a state-of-the-art production direct injection spark ignition vehicle were measured with a variety of techniques, including laser-induced incandescence. Whereas most of the techniques measure both the soot and condensed aerosols, which contribute significantly to the lack of repeatability, LII measures only the concentration of soot. The large differences in the gravimetric measurements are attributable to the poor repeatability of this method and to variation in the levels of condensed particulates. The elemental carbon measurements have been demonstrated to be the most consistent measure of particulates. From the LII results, there was a measurable increase in the soot content from Trial 1 to Trial 2. By comparing the ELPI and LII results, it is apparent that there was a significant decrease in the concentration of the organic carbon content from Trial 1 to Trial 2. This is consistent with the results obtained from the OC/EC analysis.

The soot measurements reported a new minimum threshold for LII of 5 ppt (0.01 mg/m$^3$), demonstrating the sensitivity of this technique. As expected, the highest levels of soot emissions for this DISI vehicle were recorded during the cold start phase. After the cold start period, average soot emissions were 0.2 mg/m$^3$, with peak levels all below 1 mg/m$^3$.

Both LII and ELPI demonstrated that maximum emission rates occur during acceleration transients. Steady–state driving and deceleration produce much lower levels of particulates. From the LII results, there is a clear correlation between acceleration and soot emission rates. LII demonstrated superior sensitivity to soot at the low levels observed with this vehicle, and also provided greater temporal response to variations in the soot levels.

The LII technique is capable of real-time soot measurements over all vehicle transient operations, making it a valuable tool in tuning gasoline engine soot emissions performance. The wide measurement range and low detection limit of LII make it a preferred standard instrument for soot measurements. Further development of the LII technique has the potential to give information about extensive aspects of the morphology of the particulate matter. LII also provides a significant time advantage over the gravimetric procedure, providing real-time results.

## ACKNOWLEDGMENTS

## CONTACTS

The authors Smallwood (greg.smallwood@nrc.ca), Snelling, Gülder, Clavel, Gareau, and Sawchuk are with the National Research Council Canada, ICPET Combustion Research Group, Building M-9, 1200 Montreal Road, Ottawa, Ontario K1A 0R6, Canada (www.icpet.nrc.ca/combustion), and the author Graham is with Environment Canada, Emissions Research and Measurement, 3439 River Road South, Ottawa, Ontario K1A 0H3, Canada.

## REFERENCES

1. Hansen, J., Sato, M., Reto, R., Lacis, A., and Oinas, V., "Global Warming in the Twenty-First Century: An Alternative Scenario," Proceedings of the National Academy of Sciences, 97, pp.9875-9880, 2000.
2. Jacobson, M. Z., "Strong Radiative Heating Due to the Mixing State of Black Carbon in Atmospheric Aerosols," Nature, 409, pp.695-697, 2001.
3. Kittelson, D. B., "Engines and Nanoparticles: A Review," Journal of Aerosol Science, 29, pp.575-588, 1998.
4. Witze, P. O., "Diagnostics for the Measurement of Particulate Matter Emissions from Reciprocating Engines," The Fifth International Symposium on Diagnostics and Modeling of Combustion in Internal Combustion Engines (COMODIA), Nagoya, 2001.
5. Green, R. M. and Witze, P. O., "Laser-Induced Incandescence and Elastic-Scattering Measurements of Particulate-Matter Volume Fraction Changes During Passage Through a Dilution Tunnel," Proceedings of the 10th International Symposium on Applications of Laser Techniques to Fluid Mechanics, Lisbon, July, 2000.
6. Harris, S. J., and Maricq, M. M., "Signature Size Distributions for Diesel and Gasoline Engine Particulate Matter," Journal of Aerosol Science, 32, pp.749-764, 2001.
7. Ahlvik, P., Ntziachristos, L., Keskinen, J., and Virtanen, A., "Real Time Measurements of Diesel Particulate Size Distribution with an Electrical Low Pressure Impactor," SAE Paper No. 980410, 1998.
8. Graskow, B. R., Kittelson, D. B., Ahmadi, M. R., and Morris, J. E., "Exhaust Particulate Emissions from a Direct Injection Spark Ignition Engine," SAE Paper No. 1999-01-1145, 1999.
9. Maricq, M. M., Podsiadlik, D. H., Brehob, D. D., and Haghgooie, M., "Particulate Emissions from a Direct-Injection Spark-Ignition (DISI) Engine," SAE Paper No. 1999-01-1530, 1999.
10. Hall, D. E., and Dickens, C. J., "Measurement of the Number and Size Distribution of Particles Emitted from a Gasoline Direct Injection Vehicle," SAE Paper No. 1999-01-3530, 1999.
11. Eckbreth, A. C., "Effects of Laser-Modulated Particulate Incandescence on Raman Scattering Diagnostics," Journal of Applied Physics, 48, pp.4473-4479, 1977.
12. Melton, L. A., "Soot Diagnostics Based on Laser Heating," Applied Optics, 23, pp.2201-2208, 1984.
13. Dasch, C. J., "New Soot Diagnostics in Flames Based on Laser Vaporization of Soot," 20th Symposium (International) on Combustion, The Combustion Institute, pp.1231-1237, 1984.
14. Bengtsson, P. E. and Alden, M., "Application of a Pulsed Laser for Soot Measurements in Premixed Flames," Applied Physics B (Photophysics and Laser Chemistry) B48(2), pp.155-64, 1989.
15. Dec, J. E., zur Loye, A. O., and Siebers, D. L., "Soot Distribution in a D.I. Diesel Engine Using 2-D Laser

Induced Incandescence Imaging," SAE Transactions, 100, pp.277-288, 1991.

16. Quay, B., Lee, T. W., Ni, T. and Santoro, R. J., "Spatially Resolved Measurements of Soot Volume Fraction Using Laser-Induced Incandescence," Combustion and Flame, 97, pp.384-392, 1994.

17. Vander Wal, R. L., and Weiland, K. J., "Laser-Induced Incandescence: Development and Characterization Towards a Measurement of Soot Volume Fraction," Applied Physics B, 59, pp.445-452, 1994.

18. Bengtsson, P. E., and Alden, M., "Soot Visualization Strategies Using Laser Techniques: Laser-Induced Fluorescence in $C_2$ from Laser-Vaporized Soot and Laser-Induced Soot Incandescence," Applied Physics B, 60, pp.51-59, 1995.

19. Will, S., Schraml, S., and Leipertz, A., "Two-Dimensional Soot Particle Sizing by Time-Resolved Laser-Induced Incandescence," Optics Letters, 20, pp.2342-2344, 1995.

20. Mewes, B. S., and Seitzman, J. M., "Soot Volume Fraction and Particle Size Measurements with Laser-Induced Incandescence," Applied Optics, 36, pp.709-717, 1997.

21. Snelling, D. R., Smallwood, G. J., Campbell, I. G., Medlock, J. E., and Gülder, Ö. L., "Development and Application of Laser Induced Incandescence (LII) as a Diagnostic for Soot Particulate Measurements," Proceedings of the NATO/AGARD Propulsion and Energetics Panel, 90th Symposium on Advanced Non-Intrusive Instrumentation for Propulsion Engines, 20-24 October, 1997, Brussels, Belgium.

22. Witze, P. O., Hochgreb, S., Kayes, D., Michelsen, H. A. and Shaddix, C. R., "Time-Resolved Laser-Induced Incandescence and Laser Elastic Scattering Measurements in a Propane Diffusion Flame," Applied Optics, 40, pp.2443-2452, 2001.

23. Snelling, D. R., Liu, F., Smallwood, G. J. and Gülder, Ö. L., "Evaluation of the Nanoscale Heat and Mass Transfer Model of the Laser-Induced Incandescence: Prediction of the Excitation Intensity," NHTC2000-12132, Thirty Fourth National Heat Transfer Conference, Pittsburgh, Pennsylvania, 2000.

24. Smallwood, G. J., Snelling, D. R., Liu, F. and Gülder, Ö. L., "Clouds over Soot Evaporation: Errors in Modeling Laser-Induced Incandescence of Soot," Journal of Heat Transfer, 123, pp. 814-818, 2001.

25. Vander Wal, R. L., Ticich, T. M. and Stephens, A. B., "Optical and Microscopy Investigations of Soot Structure Alterations by Laser-Induced Incandescence," Applied Physics B, 67, pp.115-123, 1998.

26. Snelling, D. R., Thomson, K. A., Smallwood, G. J. and Gülder, Ö. L., "Two-Dimensional Imaging of Soot Volume Fraction in Laminar Diffusion Flames," Applied Optics, 38, pp.2478-2485, 1999.

27. Zhao, H., and Ladommatos, N., "Optical Diagnostics for Soot and Temperature Measurement in Diesel Engines," Progress in Energy and Combustion Science, 24, pp. 221-255, 1998.

28. Schraml, S., Will, S., and Leipertz, A., "Simultaneous Measurement of Soot Mass Concentration and Primary Particle Size in the Exhaust of a DI Diesel Engine by Time-Resolved Laser-Induced Incandescence (TIRE-LII)," SAE Paper 1999-01-0146, 1999.

29. Black, J. D., "Laser Induced Incandescence Measurements of Particles in Aero-Engine Exhausts," SPIE, 3821, pp.209-215, 1999.

30. Snelling, D. R., Smallwood, G. J. and Gülder, Ö. L., "Absolute Light Intensity Measurements in Laser Induced Incandescence," US Patent No. 6,154,277, 2000.

31. Snelling, D. R., Smallwood, G. J. Gülder, Ö. L., Liu, F., and Bachalo, W. D., "A Calibration-Independent Technique of Measuring Soot by Laser-Induced Incandescence Using Absolute Light Intensity," The Second Joint Meeting of the US Sections of the Combustion Institute, Oakland, California, March 25-28, 2001.

32. Snelling, D. R., Smallwood, G. J., Gülder, Ö. L., Bachalo, W. D., and Sankar, S., "Soot Volume Fraction Characterization Using the Laser-Induced Incandescence Detection Method," Proceedings of the 10th International Symposium on Applications of Laser Techniques to Fluid Mechanics, Lisbon, July, 2000.

33. Snelling, D. R., Smallwood, G. J., Sawchuk, R. A., Neill, W. S., Gareau, D., Chippior, W. L., Liu, F., Gülder, Ö. L., and Bachalo, W. D., "Particulate Matter Measurements in a Diesel Engine Exhaust by Laser-Induced Incandescence and the Standard Gravimetric Procedure," SAE Paper No. 1999-01-3653, 1999.

34. Snelling, D. R., Smallwood, G. J., Sawchuk, R. A., Neill, W. S., Gareau, D., Clavel, D., Chippior, W. L., Liu, F., Gülder, Ö. L. and Bachalo, W. D., "In-Situ Real-Time Characterization of Particulate Emissions from a Diesel Engine Exhaust by Laser-Induced Incandescence," SAE Paper No. 2000-01-1994, 2000.

35. Smallwood, G. J., Snelling, D. R., Neill, W. S., Liu, F., Bachalo, W. D., and Gülder, Ö. L., "Laser-Induced Incandescence Measurements of Particulate Matter Emissions in the Exhaust of a Diesel Engine," The Fifth International Symposium on Diagnostics and Modeling of Combustion in Internal Combustion Engines (COMODIA), Nagoya, 2001.

36. Ü. Ö. Köylü, "Quantitative Analysis of In Situ Optical Diagnostics for Inferring Particle/Aggregate Parameters in Flames: Implications for Soot Surface Growth and Total Emissivity," Combustion and Flame, 109, pp.488-500, 1996.